sustainability

MDPI

Article

Effect of Intensifier Additives on the Performance of Butanolic Extract of Date Palm Leaves against the Corrosion of API 5L X60 Carbon Steel in 15 wt.% HCl Solution

Saviour A. Umoren *, Moses M. Solomon, Ime B. Obot and Rami K. Suleiman

Centre of Research Excellence in Corrosion, Research Institute, King Fahd University of Petroleum and Minerals, Dhahran 31261, Saudi Arabia; solomosmon2012@yahoo.com (M.M.S.); obot@kfupm.edu.sa (I.B.O.); ramismob@kfupm.edu.sa (R.K.S.)

* Correspondence: umoren@kfupm.edu.sa

Abstract: The quest to replace toxic chemicals in the nearest future is revolutionizing the corrosion inhibitor research world by turning its attention to plant biomaterials. Herein, we report the corrosion inhibiting potential of butanolic extract of date palm leaves (BUT) on the corrosion of API 5L X60 carbon steel in 15 wt.% HCl solution. The mass loss, electrochemical impedance spectroscopy (EIS), potentiodynamic polarization (PDP), linear polarization (LPR), scanning electron microscopy (SEM), energy dispersive X-ray spectroscopy (EDAX), and atomic force microscopy (AFM) techniques were employed in the investigation. We also report the effect of intensifier additives, namely formic acid (FA), potassium iodide (KI), and zinc nitrate ($Zn(NO_3)_2$) as well as temperature on the corrosion inhibiting performance of BUT. BUT exhibits inhibiting ability but the extent of inhibition is dependent on concentration, temperature, and intensifiers' concentration. At 25 °C, 200 mg/L BUT and 700 mg/L BUT protected the carbon steel surface by 50% and 88%, respectively. The addition of 3 mM FA and 5 mM KI to 200 mg/L upgraded the extract performance to 97% and 95%, respectively. $Zn(NO_3)_2$ performs poorly as an intensifier for BUT under acidizing conditions. The adsorption of BUT + FA and BUT + KI is synergistic in nature whereas that of BUT + $Zn(NO_3)_2$ drifts towards antagonistic behavior according to the calculated synergism parameter. Increase in the system temperature resulted in a slight decline in the inhibition efficiency of BUT + FA and BUT + KI but with efficiency of above 85% achieved at 60 °C. The SEM and AFM results corroborate results from the electrochemical techniques.

Keywords: acid corrosion; date palm leaves extract; corrosion inhibition; synergism; inhibition enhancement; intensifiers

Citation: Umoren, S.A.; Solomon, M.M.; Obot, I.B.; Suleiman, R.K. Effect of Intensifier Additives on the Performance of Butanolic Extract of Date Palm Leaves against the Corrosion of API 5L X60 Carbon Steel in 15 wt.% HCl Solution. *Sustainability* **2021**, *13*, 5569. https://doi.org/10.3390/su13105569

Academic Editors: Emilio Bastidas-Arteaga and Antonio Conforti

Received: 15 February 2021
Accepted: 13 May 2021
Published: 17 May 2021

1. Introduction

The oil and gas sector has maintained a significant contribution to the global economy [1]. The oil and gas exploration and production operations are on the increase [1] with the current global number of producing oil and gas wells pecked at 950,000 [2,3]. The low carbon steel, especially the API grades, are indispensable in the oil and gas exploration and production operations gaining applications as fluid transportation pipelines and storage tanks [3]. However, the susceptibility of low carbon steel to corrosion [4–6] has made the use of effective corrosion inhibitors during industrial processes like descaling, pickling, acidizing, etc. non-negotiable [7–10].

Hitherto, chemicals such as aromatic amines and their salts, chromates, dichromates, nitrates, etc. were the forefront corrosion inhibitors because of their high inhibition effectiveness [11]. However, their high toxicity level has relegated them to the backdoor and has intensified the call for green chemicals—substances with no or minimal negative effect on lives and the natural environment [12,13]. In fact, the target is to phase out toxic chemicals by 2030 [14].

Extracts of different plant parts have been examined for anticorrosion properties in diverse corrosive media with the objective of deploring them as sustainable, green, and low-cost corrosion inhibitors. Haque et al. [15] reported that *Thevetia peruviana* flower extracts at 20 mg/L acted as a potential corrosion inhibitor for mild steel in 1 M HCl solution with inhibition efficiency of 91.24%. It was found from the electrochemical studies that the *Thevetia peruviana* flower extracts acted as a mixed- and interface-type corrosion inhibitor. Results from density functional theory and molecular dynamics simulations revealed that the flower extract interacted with donor–acceptor interactions and its phytochemicals acquired a flat or horizontal orientation over the mild steel surface. Haldhar et al. [16] examined the possibility of using the leaves extract of the *Cannabis sativa* plant for the protection of low carbon steel against corrosion in acidic medium (0.5 M H_2SO_4) and reported inhibition efficiency of 97.31% by 200 mg/L of the extract. Zuo et al. [17] studied the anticorrosion effect of aqueous extract of *Lilium brownii* leaves for X70 steel in 1 M HCl solution using experimental and theoretical methods. The authors found that the leaves extract exhibited a corrosion inhibition efficiency of about 85% at 200 mg/L at tested temperatures of 298 K, 303 K, and 308 K. It was found that the extract behaved as a typical mixed-type corrosion inhibitor with physical and chemical adsorption mechanisms. *Betel* leaves extracts [18] and castor oil [19] are among the most recently reported potent corrosion inhibitors for low carbon steel. Nevertheless, a comprehensive information on plant parts extracts as metals corrosion inhibitors can be found in our review [20].

In our review on plant biomaterials as corrosion inhibitors for industrial metals [20], we noted that studies on plant biomaterials as corrosion inhibitor for low carbon steel were restrained to acid (HCl or H_2SO_4) concentrations of 1–2 M, which is typical for cleaning process [20]. In a typical acidizing condition (acid concentration $\geq$ 15 wt.%; temperature $\geq$ 60 °C), information on plant biomaterials as corrosion inhibitor was scanty. We associated the observation to the severe acidizing conditions, which plant biomaterials might not withstand. Considering the numerous advantages of plant biomaterials (availability, low-cost, biodegradability, environmental friendliness, sustainability, etc.), it will be reasonable to devise a mean of boosting their inhibition performance in order to expand their application areas.

Synergism, which is defined as a combined action of compounds greater in total effect than the sum of the individual effects [21] has become an important effect in inhibition process and is the basis for most modern corrosion inhibitor formulations [21]. Normally, an intensifier also known as inhibitor aid [22] or synergist [23] is added to an inhibitor to upgrade its performance [23–25]. Common synergists include formic acid [26,27] (used at a concentration range of 0.5 to 10 wt.% [22]), potassium iodide [10,22,28] (used at a concentration range of 0.5 to 10 wt.% [22]), copper halides [22], and metals ions (e.g., $Zn(NO_3)_2$, Sb_2O_3, $SbCl_3$, Sb_2O_5, etc.) [22,29,30], which are used at the concentration range of 1–1.5 wt.% [22]. This work was thus designed to examine the effect of the addition of different concentrations of $Zn(NO_3)_2$, KI, and formic acid on the corrosion inhibition performance of butanolic extract of date palm leaves for API 5L X60 carbon steel in 15 wt.% HCl solution at 25–60 °C. To accomplish this task, the mass loss, electrochemical (electrochemical impedance spectroscopy (EIS), potentiodynamic polarization (PDP), and linear polarization resistance (LPR)), and surface screening (scanning electron microscopy (SEM), energy dispersive spectroscopy (EDAX), and atomic force microscopy (AFM)) techniques were deployed for anticorrosion studies.

Date palm (*P. dactylifera*) is a flowering plant that belongs to the family of *Arecaceae* and mostly grown in the Middle East [31]. In the Kingdom of Saudi Arabia, its cultivation is covering over 170,000 hectares with total number of palms exceeding 25 million [31]. Hence, date palm has a huge potential of becoming an important raw material for various sectors. The fruits are known for its out-of-hand consumption to processing into edible and non-edible products [31–33]. There are, however, no known economic uses of the leaves. Thus, we seek to convert the non-usable date palm leaves to an economic raw material.

2. Experimental Descriptions

2.1. Leaves Collection, Preparation, and Extraction

Fresh date palm leaves were collected from the King Fahd University of Petroleum and Minerals garden. The validation of the leaves was completed by Dr. Jacob Thomas of King Saud University, Riyadh, Saudi Arabia. The deposited date palm leaves sample in King Saud University herbarium is assigned KSU No. 22,638 as identification number. After identification, the leaves were sliced, washed with distilled water, sun dried for 2 weeks, and ground into powder.

A total of 10 g of the leaves' powder was accurately weighed, soaked in 250 mL of butanol at room temperature, and stirred at 300 rpm continuously for 72 h. The butanol–leaf powdered mixture was filtered using ADVANTEC® No. 1 filter papers (90 mm size) and the filtrate concentrated in a rotary evaporator to a semi-solid form. The concentrated semi-solid was left in the fume extraction booth overnight and the solid extract obtained was weighed to determine the amount (1.5529 g) extracted. The butanolic date palm leaves extract is herein abbreviated as BUT extract.

2.2. Metal Specimen Composition, Preparation, and Corrosive Medium

The chemical composition of the API 5L X60 carbon steel is as previously reported [6]. The procedure followed in sample pre-treatment was as listed in ASTM G1-90 procedure [34]. Mechanical abrasion was done with the help of Buchler CarbiMet^{TM} papers up to 1000-grit. The corrosive solution was 15 wt.% HCl prepared by diluting appropriate amount of analytical grade hydrochloric acid (37%, Merck) with double distilled water.

2.3. Corrosion Testing Experiments

Mass loss experiments were carried out following the NACE TM0169/G31 [35] procedure. Summarily, the initial mass (M_0) of the completely abraded X60 coupons (dimension = 2.97 cm × 2.86 cm × 1.10 cm; surface area = 30 cm^2) was measured. Two coupons each were freely suspended in 250 mL capacity reaction bottles filled with 200 mL of respective test solutions (15 wt.% HCl solutions uninhibited and inhibited with 200 mg/L BUT, 200 mg/L BUT + 5 mM KI, 200 mg/L BUT + 1 mM $Zn(NO_3)_2$, and 200 mg/L + 3 mM FA) such that the samples were completely submerged. Herein, the uninhibited 15 wt.% HCl solution is referred to as 'blank' while the acid solution containing the additives is referred to as 'inhibited'. The reaction bottles were placed in a Thermo Scientific precision water bath maintained at studied temperatures (25, 40, 50, and 60 °C) for 24 h. Thereafter, the coupons were removed from the test solutions and post-treated following the procedure detailed in the ASTM G1-90 standard [34]. That is, the corroded specimens were dipped in 1 M HCl solution for 20 s, washed in distilled water and ethanol thoroughly, and dried in warm air (about 40 °C) for 5 min. Thereafter, the mass of the post-treated coupons was measured and labelled as M_1. The mass loss was then calculated using Equation (1).

$$\text{Mass loss (g)} = M_0 - M_1 \tag{1}$$

The corrosion rate (v) in g/cm^2 h and the percentage inhibition efficiency (η) were calculated using Equations (2) and (3), respectively [36].

$$v = \frac{\overline{M}}{At} \tag{2}$$

$$\eta = \left(\frac{\overline{M}_{\text{blank}} - \overline{M}_{\text{inhibited}}}{\overline{M}_{\text{blank}}} \right) \times 100 \tag{3}$$

$\overline{M}$ is the mean mass loss, A is the exposed surface area, and t is the immersion time.

All electrochemical experiments were done in a Gamry Potentiostat/Galvanostat/ZRA Reference 600 instrument adopting the ASTM G3-89 [37] and G3-94 [38] standard procedures. The volume of test solution utilized in these sets of experiments was 150 mL.

An epoxy-encapsulated API 5L X60 carbon steel with exposed area of 0.73 cm^2 was the working electrode while a graphite rod and silver/silver chloride (sat. KCl, 4.2 M) electrode played the roles of a counter electrode and reference electrodes, respectively. Prior to electrochemical impedance spectroscopy (EIS) experiments, the open circuit potential (OCP) of the corroding system was monitored for 3600 s to ensure a steady-state condition. The EIS experimental parameters used were: initial frequency = 100,000 Hz, final frequency = 0.01 Hz, amplitude signal = 10 mV acquiring 10 points/decade at OCP. For the linear polarization (LPR) experiments, set-up parameters were: initial potential = −15 mV and final potential = +15 mV versus open circuit potential at the scan rate of 0.125 mV s^{-1}. The potentiodynamic polarization (PDP) experiments were conducted at a scan rate of 0.2 mV/s from −250 mV to +250 mV versus open circuit potential. All the experiments exception of the OCP and PDP were repeated 3 times to ensure reproducibility. The EIS and LPR data were analyzed using an Echem analyst while EC-lab software was used for PDP data analysis. The percentage inhibition efficiency from PDP technique was computed using Equation (4) while that from EIS and LPR technique was calculated using Equation (5) [39].

$$\eta = \left(\frac{\bar{i}_{\text{blank}} - \bar{i}_{\text{inhibited}}}{\bar{i}_{\text{blank}}} \right) \times 100 \quad (4)$$

$$\eta = \left(\frac{\overline{R_{\text{P}}}_{\text{inhibited}} - \overline{R_{\text{P}}}_{\text{blank}}}{\overline{R_{\text{P}}}_{\text{inhibited}} } \right) \times 100 \quad (5)$$

where $\bar{i}$ and $\overline{R_{\text{p}}}$ are the mean current density and polarization resistance, respectively.

The surface morphologies of the corroded API 5L X60 carbon steel samples exposed to the uninhibited and inhibited 15 wt.% HCl solution for 24 h were observed using a scanning electron microscope (SEM), JEOL JSM-6610 LV model coupled to energy dispersive X-ray spectroscopy (EDAX) for chemical composition determination. AFM measurements were done using a 5420 atomic force microscope (N9498S, Agilent Technologies, UK) operated in the contact mode under ambient conditions. Unlike the samples for SEM and EDAX analysis, the samples for AFM analysis, after removing from the test solutions were carefully washed in running water and ethanol, dried in warm air for 5 min before submitting for the analysis. This was to eliminate the effect of adsorbed products on the roughness property of the surface.

3. Results and Discussion

3.1. Corrosion Inhibition of BUT

The corrosion inhibition of API 5L X60 carbon steel in 15 wt.% HCl solution by BUT and the effect of varying concentration on the inhibition was studied using the EIS, LPR, and the PDP techniques. The impedance and the polarization graphs obtained from the studies are displayed in Figure 1a,b, respectively. It is obvious from Figure 1a,b that the presence of BUT in the corrosive solution had corrosion inhibiting effect. The appearance of a depressed semicircle with larger diameter (Figure 1a) and the suppression of the corrosion current density (Figure 1b) in the presence of BUT are indicators of API 5L X60 corrosion inhibition [30]. The corrosion inhibition performance by BUT is found to improve with increasing concentration with the largest semicircle (Figure 1a) and the lowest corrosion current density (Figure 1b) produced by the highest studied BUT concentration (700 mg/L). The LPR results shown in Figure 1c reveals that, the polarization resistance of the carbon steel sample in the HCl solution and the inhibition efficiency of BUT steadily increased with increase in BUT concentration. The polarization resistance of the steel sample in the uninhibited corrosive solution (15 wt.% HCl) is 62.27 ± 2.20 Ω cm^2 but 122.40 ± 1.40 Ω cm^2, 244.90 ± 0.60 Ω cm^2, and 432.20 ± 2.09 Ω cm^2 in 200 mg/L, 500 mg/L, and 700 mg/L BUT inhibited systems, respectively. The inhibition efficiency increased from 49.12% at BUT concentration of 200 mg/L to 74.57% and 85.59%, respectively, at BUT concentration of 500 mg/L and 700 mg/L. These observations could be due to the adsorption of some

molecules of phytochemicals present in BUT on the steel surface that obstructed the charge transfer processes on the steel surface [30,40,41].

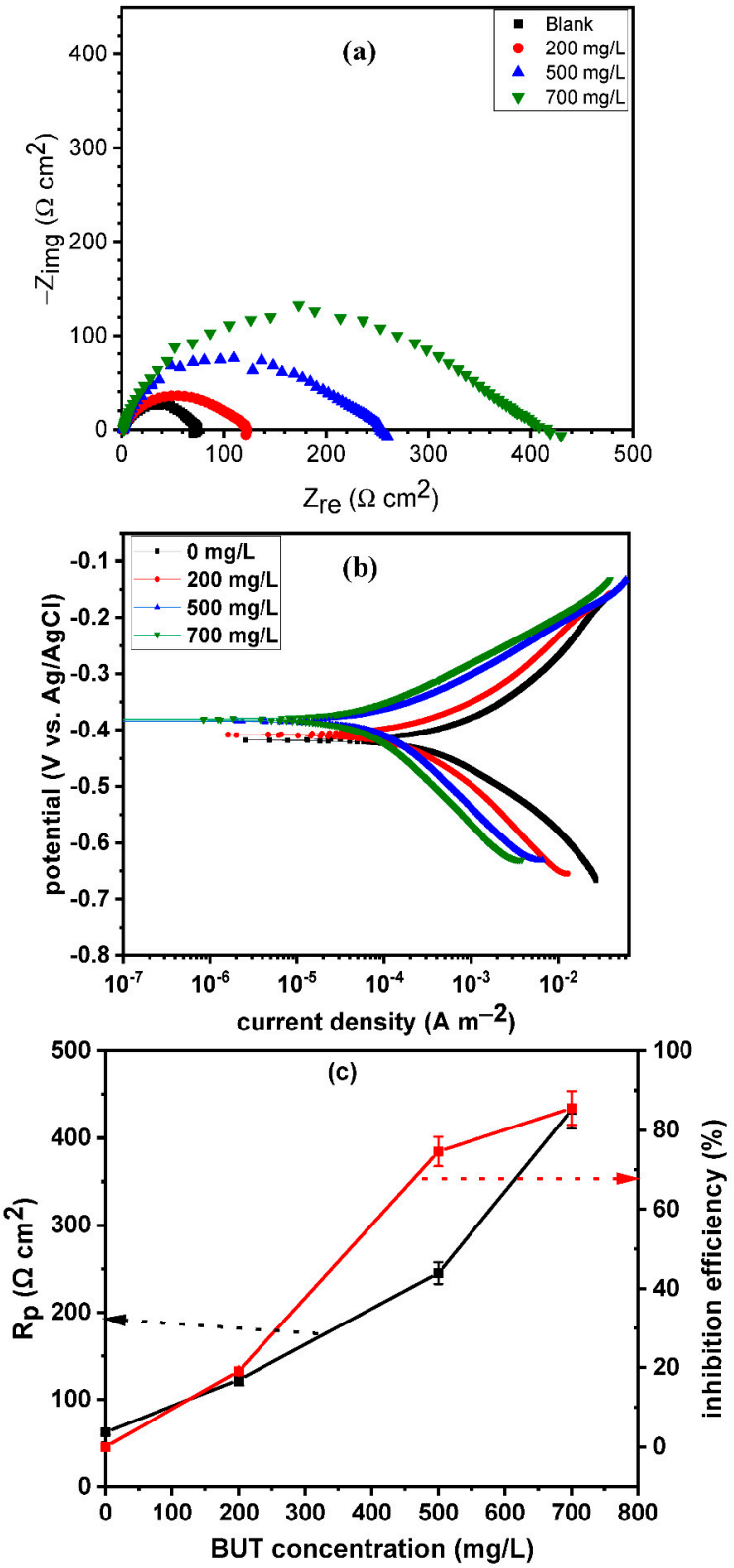

Figure 1. (**a**) Impedance, (**b**)potentiodynamic polarization, and (**c**) polarization resistance and inhibition efficiency from LPR measurements plots for API 5L X60 carbon steel at 25 °C in 15 wt.% HCl solution without and with different concentrations of BUT.

The double layer capacitance (C_{dl}) is an important parameter, which can provide insight into adsorption process [30,41]. For a corrosion system driven by charge transfer process and diffusion is excluded, C_{dl} can be calculated using the Brug's formula [42]:

$$C_{\mathrm{dl}} = {Y_{dl}}^{1/n}\left(\frac{1}{R_s} + \frac{1}{R_{ct}}\right)^{\frac{(n-1)}{n}} \quad (6)$$

where R_s is the solution resistance, R_{ct} is the charge transfer resistance, Y_{dl} is the constant phase element (CPE) constant, and n is the CPE exponent. The numerical values of these parameters (R_s, R_{ct}, Y_{dl}, and n) as listed in Table 1 were obtained by fitting the impedance data into a simple equivalent circuit (EC). The diagram of the EC has already been given in our previous publication [43]. The inhibition efficiency values also given in Table 1 were calculated using Equation (5) but with $\overline{R_{\mathrm{p}}}$ replaced with $\overline{R_{\mathrm{ct}}}$. A smaller value of C_{dl} is noted for the inhibited systems compared to the uninhibited (Table 1). In addition, a decreasing trend with increasing BUT concentration is also observed for C_{dl} in the table. The Helmholtz model (Equation (7)) makes these observations more meaningful. According to the Helmholtz model, at constant surface area, a change in the local dielectric constant and in the thickness of surface film can affect C_{dl}. It can be claimed that the observed smaller value of C_{dl} for inhibited systems relative to uninhibited system is due to the lowering of the local dielectric constant caused by the substitution of adsorbed water molecules on the metal surface by the inhibitor molecules [44] while the decrease in C_{dl} value with increasing BUT concentration is due to an increase in the thickness of the electrical double layer [43]. This claim is also supported by the increasing trend in the R_{ct} (Table 1), R_p (Figure 1c), and inhibition efficiency (Table 1) values with increasing extract concentration. The Y_{dl} value, which provides information on the characteristics of the adsorbed films on the API 5L X60 carbon steel surface reveals that the inhibitor film was more compact than the corrosion product film, i.e., the Y_{dl} value for the blank is much higher than that of the inhibited surfaces [45].

$$C_{dl} = \frac{\varepsilon_0 \varepsilon}{d} S \quad (7)$$

where ε_0 is the permittivity of air, ε is the local dielectric constant, d is the adsorbed film thickness, and S is the electrode surface area.

Table 1. EIS parameters obtained during acid corrosion of API 5L X60 carbon steel in 15 wt.% HCl solution without and with various additives at 25 °C.

System	R_s (Ω cm^2)	CPE_{dl}		R_{ct} (Ω cm^2)	C_{dl} (μF cm^{-2})	x^2 ($\times 10^{-4}$)	% η_{EIS}
		Y_{dl} (μF cm^{-2} s^{n-1})	n_{dl}				
BUT extract							
0 ppm	2.07 ± 0.03	222.00 ± 0.00	0.87 ± 0.01	69.36 ± 2.44	70.05	3.31	–
200 ppm	1.61 ± 0.02	151.00 ± 0.00	0.82 ± 0.01	117.65 ± 1.51	24.20	8.66	41.00
500 ppm	1.34 ± 0.02	54.38 ± 0.00	0.87 ± 0.01	258.70 ± 0.59	13.08	3.98	73.20
700 ppm	1.92 ± 0.03	55.50 ± 0.00	0.86 ± 0.01	394.20 ± 2.40	12.51	1.56	82.40
Synergist							
1 mM FA	1.20 ± 0.12	231.70 ± 0.00	0.84 ± 0.01	74.29 ± 4.18	48.55	2.38	6.64
3 mM FA	1.20 ± 0.17	125.90 ± 0.00	0.90 ± 0.17	157.69 ± 0.61	41.49	3.28	56.01
5 mM FA	1.20 ± 0.18	123.60 ± 0.00	0.89 ± 0.11	109.85 ± 1.00	47.32	2.33	36.86
1 mM KI	1.36 ± 0.14	141.70 ± 0.00	0.88 ± 0.00	120.20 ± 0.63	44.07	5.02	42.30
3 mM KI	1.30 ± 0.01	116.40 ± 0.00	0.88 ± 0.00	141.70 ± 0.73	35.03	13.94	51.05
5 mM KI	4.30 ± 0.03	87.40 ± 0.00	0.88 ± 0.00	173.60 ± 0.92	29.72	10.04	60.05
1 mM $Zn(NO_3)_2$	1.23 ± 0.01	183.70 ± 0.00	0.87 ± 0.00	84.22 ± 9.33	52.26	1.34	17.64
3 mM $Zn(NO_3)_2$	1.41 ± 0.01	195.20 ± 0.00	0.88 ± 0.00	82.98 ± 7.08	63.64	2.09	16.41
5 mM $Zn(NO_3)_2$	1.40 ± 0.01	220.80 ± 0.00	0.86 ± 0.00	86.90 ± 6.98	59.06	1.47	20.18

The relevant polarization parameters, namely corrosion potential (E_{corr}), corrosion current density (i_{cor}), anodic and cathodic Tafel slope (β_a, β_c) obtained from the analyses of Figure 1b are summarized in Table 2. Inhibition efficiency values from this technique were calculated using Equation (4). The numerical values of E_{corr} listed in Table 2 are consistent with the visual observation of Figure 1b. That is, there is a shift in corrosion potential upon introduction of BUT into the corrosive medium but the shift is insignificant. The highest displacement is noticed in 700 mg/L BUT containing solution whereby the E_{corr} is changed from −418 mV/Ag/AgCl to −381 mV/Ag/AgCl. This behavior is indicative of BUT behaving as a mixed-type corrosion inhibitor impeding both the anodic and cathodic reactions [41] but with slight anodic preference. Compared to the blank, there is a significant decrease in i_{corr} of the BUT inhibited corrosive medium. The i_{corr} value diminished from 514.85 μA cm^{-2} recorded in the unprotected acid medium to 255.60 μA cm^{-2} in the system inhibited with 200 mg/L BUT. This translated to a corrosion inhibition of 50.35%. Increase in the dosage of the extract to 500 mg/L and 700 mg/L further brought down the i_{corr} to 102.07 μA cm^{-2} and 62.16 μA cm^{-2} resulting in corrosion protection of 80.17% and 87.93%, respectively. This further demonstrates the effectiveness of BUT as acid corrosion inhibitor. Furthermore, the numerical values of β_a and β_c reveal that there is no significant variation in the β_a and β_c values with increasing BUT concentration. That is, the change in β_a and β_c values with increase in BUT concentration is minimal. A similar observation was reported by Kousar et al. [41] and is suggestive of non-alteration in the inhibition mechanism of the anodic and cathodic corrosion reactions. It suggests that the inhibition of API 5L X60 carbon steel in 15 wt.% HCl solution by BUT is achieved by active anodic and cathodic sites blockage. Interface inhibitors, as it is known can inhibit corrosion by [46,47]: (i) geometric blockage effect, i.e., the inhibition effect comes from the reduction of the reaction area on the surface of the corroding metal [48], (ii) active site blockage, or (iii) electro-catalytic effect. Inhibition by active site blockage and electro-catalytic effect are believed to be due to changes in the average activation energy barriers of the anodic and cathodic reactions of the corrosion process [48]. The prevalence mechanism can be deduced by calculating the coefficients of anodic (f_a) and cathodic (f_c) reactions [46]. If inhibition is by geometrical blocking, f_a is equals to f_c [46] and the difference between the corrosion potential of inhibited and uninhibited systems (ΔE_{corr}) is zero [48]. For corrosion inhibition achieved by active site blocking, f_a and f_c are less than unity whereas f_a or f_c is greater than unity for corrosion inhibition through electro-catalytic effect [46]. In the latter case, a noticeable difference exist in ΔE_{corr} [48]. For the system under consideration, the calculated values of f_a and f_c (Equations (8) and (9)) [46] listed in Table 2 fall under the second category pointing to inhibition by anodic and cathodic active corrosion sites blockage by adsorbed phytochemical molecules present in BUT. The noticeable shift in the corrosion potential of the inhibited systems relative to the uninhibited also support inhibition by active site blockage [48]. Arellanes-Lozada et al. [46] had reported the inhibition of API 5L X52 steel corrosion in acid medium by 1-butyl-2,3-dimethyl-imidazolium iodide and 1-propyl-2,3-dimethyl-imidazolium iodide by active sites blocking mechanism. Finally, it is worth pointing out that the inhibition efficiency values obtained from the different electrochemical techniques (Tables 1 and 2) are in good agreement.

$$f_a = \left(\frac{i_{corr}^{inhibited}}{i_{corr}^{blank}}\right) e^{\frac{E_{corr}^{blank} - E_{corr}^{inhibited}}{\beta_a}} \quad (8)$$

$$f_c = \left(\frac{i_{corr}^{inhibited}}{i_{corr}^{blank}}\right) e^{\frac{E_{corr}^{blank} - E_{corr}^{inhibited}}{\beta_c}} \quad (9)$$

Table 2. Polarization parameters obtained during acid corrosion of API 5L carbon steel in 15 wt.% HCl solution without and with various additives at 25 °C.

Conc. (ppm)	LPR		PDP						
	Rp (Ω cm^2)	% η_{LPR}	$-E_{corr}$ (mV/Ag/AgCl)	i_{corr} (μA cm^{-2})	β_a (mV dec^{-1})	$-\beta_c$ (mV dec^{-1})	f_a	f_c	% η_{PDP}
BUT extract									
0	–	–	418	514.85	106.80	123.80	-	-	–
200	–	–	416	255.60	107.00	122.10	0.51	0.50	50.35
500	–	–	384	102.07	85.80	153.60	0.29	0.24	80.17
700	–	–	381	62.16	82.20	154.60	0.19	0.15	87.93
Synergist									
1 mM FA	70.01 ± 2.20	11.06	416	431.30	117.70	122.40	0.85	0.85	16.23
3 mM FA	152.10 ± 0.60	59.06	397	230.24	100.40	120.10	0.55	0.53	55.28
5 mM FA	106.70 ± 2.60	41.64	397	296.37	115.00	124.00	0.69	0.68	42.44
1 mM KI	107.80 ± 1.40	42.24	418	292.14	108.00	122.40	0.57	0.57	43.26
3 mM KI	124.50 ± 1.70	49.98	414	247.03	87.20	112.90	0.50	0.50	52.02
5 mM KI	131.00 ± 3.21	52.46	411	238.10	67.90	88.60	0.51	0.50	53.75
1 mM $Zn(NO_3)_2$	75.82 ± 0.09	17.87	417	420.86	109.30	122.60	0.82	0.82	18.26
3 mM $Zn(NO_3)_2$	77.55 ± 1.22	19.70	412	415.14	129.40	121.70	0.84	0.85	19.37
5 mM $Zn(NO_3)_2$	74.90 ± 1.72	16.86	417	422.69	130.40	130.50	0.83	0.83	17.90

3.2. Effect of Intensifier Additives on the Corrosion Inhibition of BUT

An important aspect always considered when formulating a corrosion inhibitor cocktail (a mixture containing an active, intensifier, surfactant, solvent, co-solvent, etc.) is how to achieve adequate corrosion inhibition at a low cost. The use of intensifiers in inhibitor cocktail is sacrosanct since a single molecule barely achieve a desired inhibition [22]. The role of an intensifier is to enhance the inhibitive force of the active [22] and as a consequent decrease the amount of active used [49]. Formic acid (FA), potassium iodide (KI), and zinc nitrate ($Zn(NO_3)_2$) are some commonly used intensifiers [12,26,27,29,30]. Theoretically, FA aids corrosion inhibition by undergoing a dehydration reaction to form water and carbon monoxide ($HCOOH \rightarrow CO + H_2O$) [26,27]. The CO is believed to adsorb onto a metal surface forming a strong nonpolar bond [26,27]. This theory has been verified experimentally by corrosion scientists [26,27]. Nevertheless, FA does not spontaneously decompose in any condition but requires a strong acid solution and heat [27]. For KI, the prevailing theory is that, in acid solution, dissolved oxygen oxidizes iodide ions to triiodide and pentaiodide ions, which are preferentially adsorbed on metal surface [39,50]. The oxidation of iodide ions to triiodide and pentaiodide ions had been demonstrated through the use of X-ray photoelectron spectroscopy [39,50]. Zn^{2+}, which is the most investigated cation for synergistic effect with metal corrosion inhibitors [11] is believed to easily form Zn^{2+}-inhibitor complex in solution. Upon immersion of a metal higher up in the electrochemical series than Zn, the Zn^{2+}-inhibitor complex is believed to diffuse to the substrate surface and converted to a stable metal–inhibitor complex in the local anodic region [11] while the freed Zn^{2+} ion forms $Zn(OH)_2$ precipitate in the local cathodic region ($Zn^{2+} + 2OH^- \rightarrow Zn(OH)_2$) [11].

Figure 2 shows the electrochemical and polarization curves for API 5L X60 carbon steel at 25 °C in 15 wt.% HCl solution without and with different concentrations of (a, b) FA, (c, d) KI, and (e, f) $Zn(NO_3)_2$ alone. The electrochemical and polarization parameters obtained from the analysis of the data are also listed in Table 2. These sets of experiments were carried out to understand the extent to which the selected intensifiers alone can inhibit

the corrosion of the carbon steel. The concentration was varied so as to determine the optimum concentration for the studied experimental conditions. It is clear from Figure 2 and Table 2 that the selected intensifiers exhibit inhibitory property to a certain degree. For FA, the 3 mM concentration seems to be the optimum concentration exhibiting inhibition efficiency in the range of 55.28–59.06% (Table 2). The best concentration for KI is 5 mM and this concentration afforded inhibition efficiency in the range of 52.24–53.75% (Table 2). For $Zn(NO_3)_2$, the corrosion inhibition performance of the three concentrations is very close and should be of benefit to use the low concentration. However, among the three intensifiers, $Zn(NO_3)_2$ exhibited the least corrosion inhibition performance. For example, the inhibition efficiency afforded by 3 mM $Zn(NO_3)_2$ is 16.41% from EIS technique whereas 3 mM FA and 3 mM KI protected the carbon steel surface by 56.01% and 51.05%, respectively. This seems to suggest that $Zn(NO_3)_2$ is not suitable as intensifier under the studied conditions.

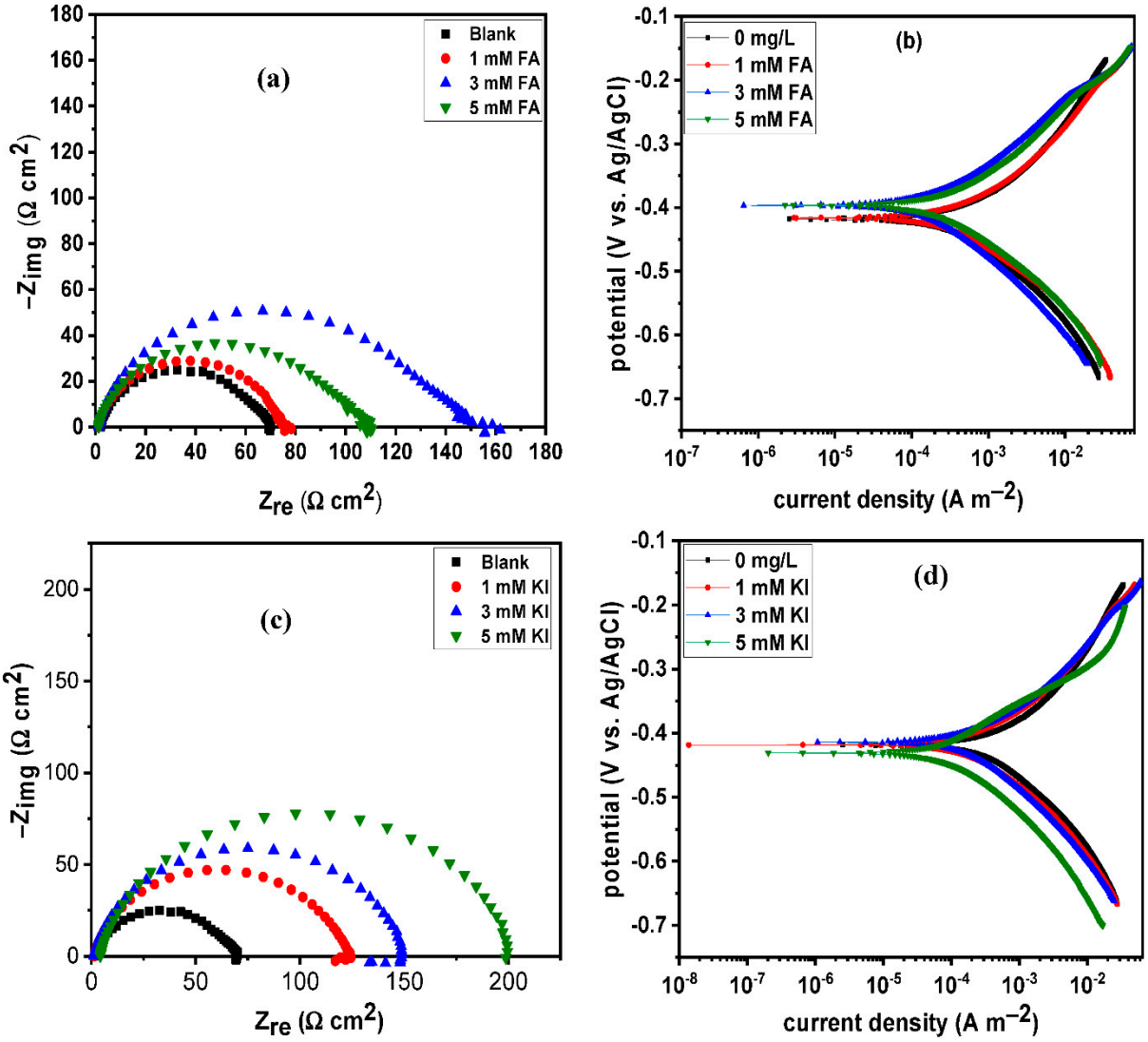

Figure 2. *Cont.*

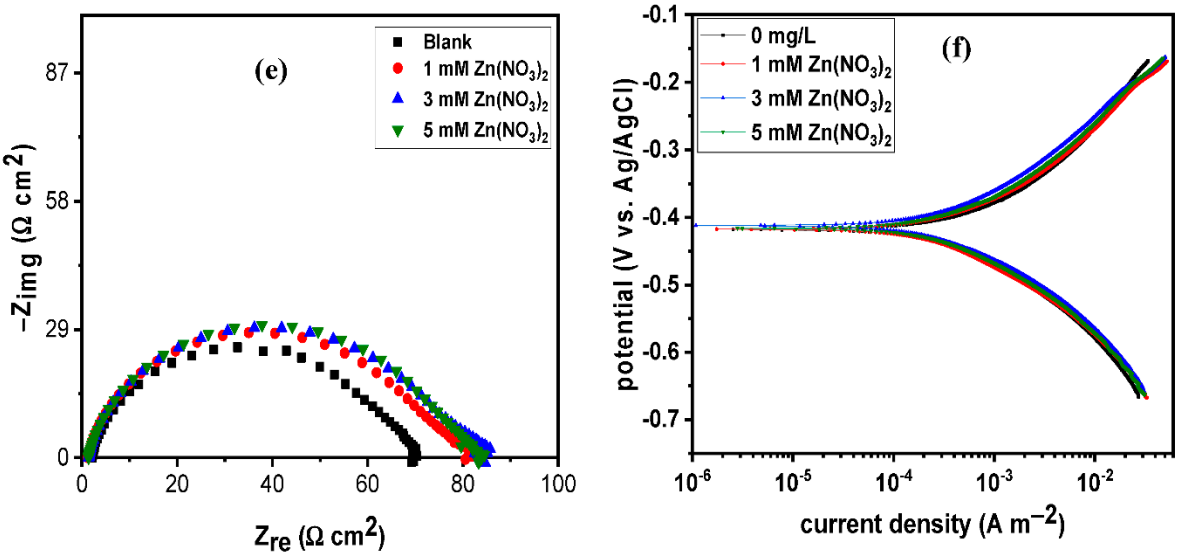

Figure 2. Electrochemical impedance and potentiodynamic polarization plots for API 5L X60 carbon steel at 25 °C in 15 wt.% HCl solution without and with different concentrations of (**a**,**b**) formic acid (FA), (**c**,**d**) potassium iodide (KI), and (**e**,**f**) zinc nitrate ($Zn(NO_3)_2$).

Although BUT at a concentration of 700 mg/L could afford corrosion inhibition up to 80% (Tables 1 and 2), it will be profitable if the amount is decreased but high inhibition performance retained. With this in mind, the various concentrations of the intensifiers were added to the least studied concentration of BUT (200 mg/L), which alone only afforded inhibition of about 50% (Tables 1 and 2). Figure 3 shows the comparative electrochemical impedance spectra for 200 mg/L BUT alone and in combination with different concentrations of the studied intensifiers. The derived EIS parameters are summarized in Table 3. In the Nyquist graphs (Figure 3), the semicircles of the BUT + intensifiers are remarkably larger than the impedance semicircles of BUT and intensifiers alone. This is indicative of better corrosion inhibition by the mixtures relative to their independent performances. Inspection of Figure 3a discloses that the BUT + 1 mM $Zn(NO_3)_2$ produced the best enhancement effect in comparison to the effect of BUT + 3 mM $Zn(NO_3)_2$ and BUT + 5 mM $Zn(NO_3)_2$. This may be caused by the saturation of the system containing BUT + 3 mM $Zn(NO_3)_2$ and BUT + 5 mM $Zn(NO_3)_2$ mixtures, which in turn caused adsorbed inhibitor species to interact with free molecules leading to film desorption and in extension, decline in inhibition efficiency (Table 3) [9]. It may also signal a competitive adsorption between BUT and Zn^{2+} ions, the so-called antagonistic adsorption [49].

In Figure 3b,c, the 5 mM KI and 3 mM FA are seen to produce an astonishing intensifying effect on the inhibition efficacy of BUT. The results in Table 3 reveals that the combination of 5 mM KI and 3 mM FA with 200 mg/L BUT boosted the inhibiting ability of BUT by 55% and 56%, respectively. That is, the inhibition efficiency of 200 mg/L BUT is upgraded from 41.00% to 90.94% and 92.54%, respectively. In fact, the inhibition performances of these mixtures are better than that of 700 mg/L of BUT (Table 1), inferring that this modification approach is profitable. The comparative graphs of the best performing combination of the intensifiers given in Figure 3d rules out $Zn(NO_3)_2$ as intensifier for BUT in an acidizing environment. As could be seen in the figure, the performance of BUT + 1 mM $Zn(NO_3)_2$ falls far behind that of BUT + 5 mM KI and BUT + 3 mM FA.

Figure 4 presents the various potentiodynamic polarization curves for API 5L X60 carbon steel at 25 °C in 15 wt.% HCl solution without and with the best performing concentration of intensifier, 200 mg/L BUT alone and in combination with different concentrations of (a) $Zn(NO_3)_2$, (b) KI, and (c) (FA). The comparison of the best BUT + intensifier combination is shown in Figure 3d. The associated polarization parameters alongside the parameters derived from LPR experiments are equally given in Table 4. Clearly, the various mixtures acted as a mixed type corrosion inhibitor displacing both the anodic and cathodic

current densities toward lower values compared to BUT alone. The f_a and the f_c values in Table 4 disclose that the mechanism of corrosion inhibition by BUT, that is active site blocking did not change upon combination with the various intensifiers. Rather, the addition of the intensifier to the extract resulted in a remarkable reduction in the i_{corr}, increase in R_p, and upgrading of inhibition efficiency (Table 4). For the two best combinations, BUT + 5 mM KI and BUT + 3 mM FA, the inhibition efficiency of 94.96% and 96.90% were achieved from PDP technique. The fact that the inhibition efficiency obtained from all the applied methods for BUT + 5 mM KI and BUT + 3 mM FA combinations exceeds 90% (Tables 3 and 4) portrays this modification approach as effective and benefiting.

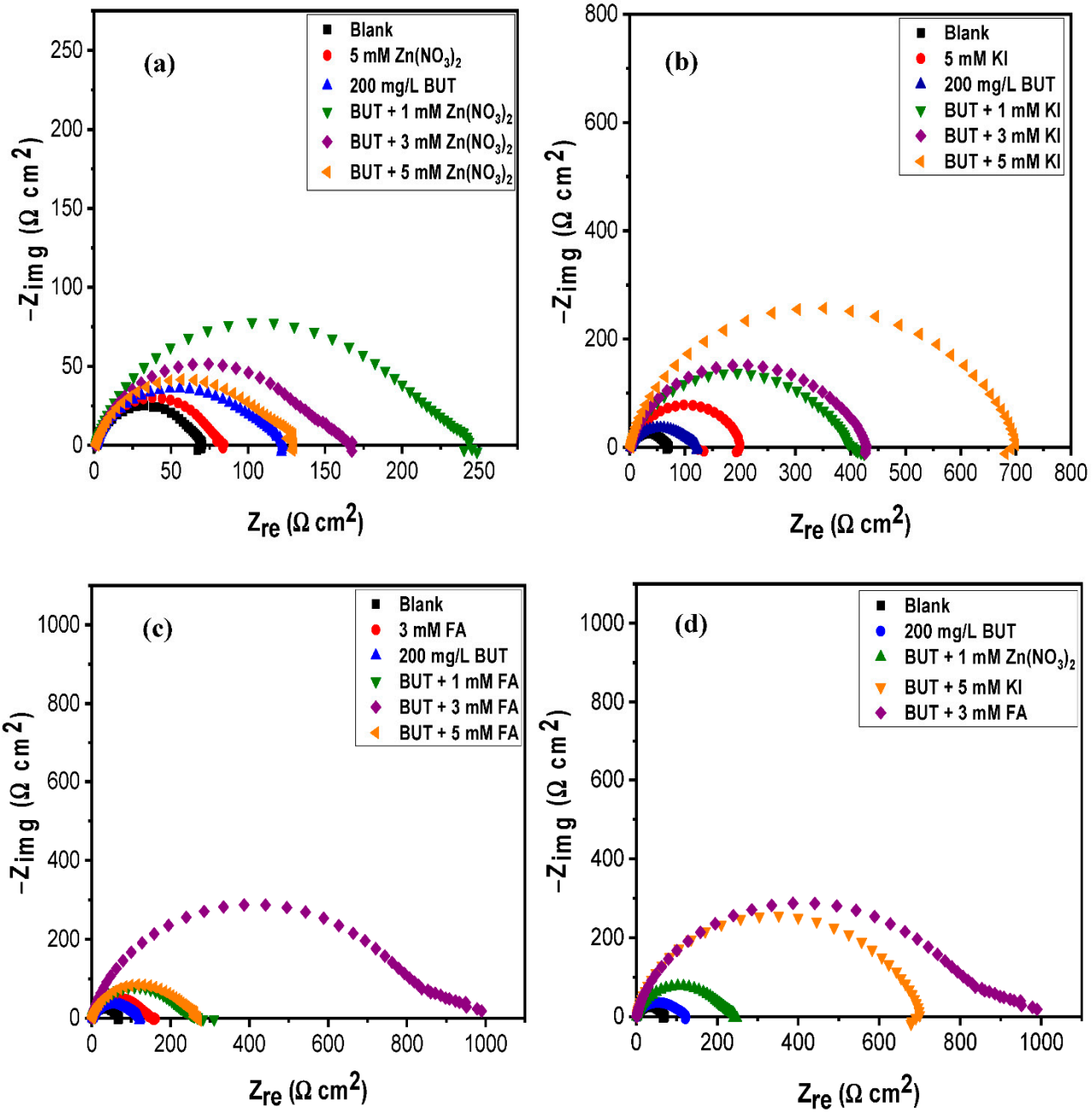

Figure 3. Impedance plots for API 5L X60 carbon steel at 25 °C in 15 wt.% HCl solution without and with best performing concentration of synergist, 200 mg/L BUT alone and in combination with different concentrations of (**a**) $Zn(NO_3)_2$, (**b**) KI, (**c**) formic acid (FA) and (**d**) comparison of the best BUT + synergist combination

Table 3. EIS parameters obtained during acid corrosion of API 5L carbon steel in 15 wt.% HCl solution without and with 200 ppm BUT alone and in combination with different synergists at 25 °C.

System	R_s (Ω cm^2)	CPE_{dl}		R_{ct} (Ω cm^2)	C_{dl} (μF cm^{-2})	x^2 ($\times 10^{-4}$)	% η_{EIS}
		Y_{dl} (μF cm^{-2} s^{n-1})	n_{dl}				
200 ppm BUT	1.61 ± 0.02	151.00 ± 0.00	0.82 ± 0.01	117.65 ± 1.51	24.20	8.66	41.00
BUT + 1 mM FA	1.22 ± 0.03	129.90 ± 0.00	0.82 ± 0.00	227.00 ± 3.17	19.01	27.46	73.37
BUT + 3 mM FA	1.18 ± 0.02	52.72 ± 0.00	0.85 ± 0.00	810.10 ± 10.88	9.54	47.39	92.54
BUT + 5 mM FA	1.23 ± 0.03	124.30 ± 0.00	0.82 ± 0.00	242.00 ± 3.46	18.05	17.18	75.02
BUT + 1 mM KI	1.61 ± 0.03	75.54 ± 0.00	0.85 ± 0.00	387.40 ± 5.06	15.38	25.42	84.40
BUT + 3 mM KI	1.57 ± 0.03	64.19 ± 0.00	0.86 ± 0.00	408.90 ± 4.55	14.34	22.23	85.22
BUT + 5 mM KI	1.65 ± 0.03	43.39 ± 0.00	0.87 ± 0.00	667.30 ± 7.32	10.42	21.47	90.94
BUT + 1 mM $Zn(NO_3)_2$	1.00 ± 0.02	139.20 ± 0.00	0.82 ± 0.00	220.70 ± 3.14	19.80	17.34	72.61
BUT + 3 mM $Zn(NO_3)_2$	1.03 ± 0.02	204.00 ± 0.00	0.81 ± 0.00	146.00 ± 2.01	27.94	12.12	58.60
BUT + 5 mM $Zn(NO_3)_2$	1.31 ± 0.02	226.00 ± 0.00	0.81 ± 0.00	120.30 ± 1.91	33.52	12.49	49.76

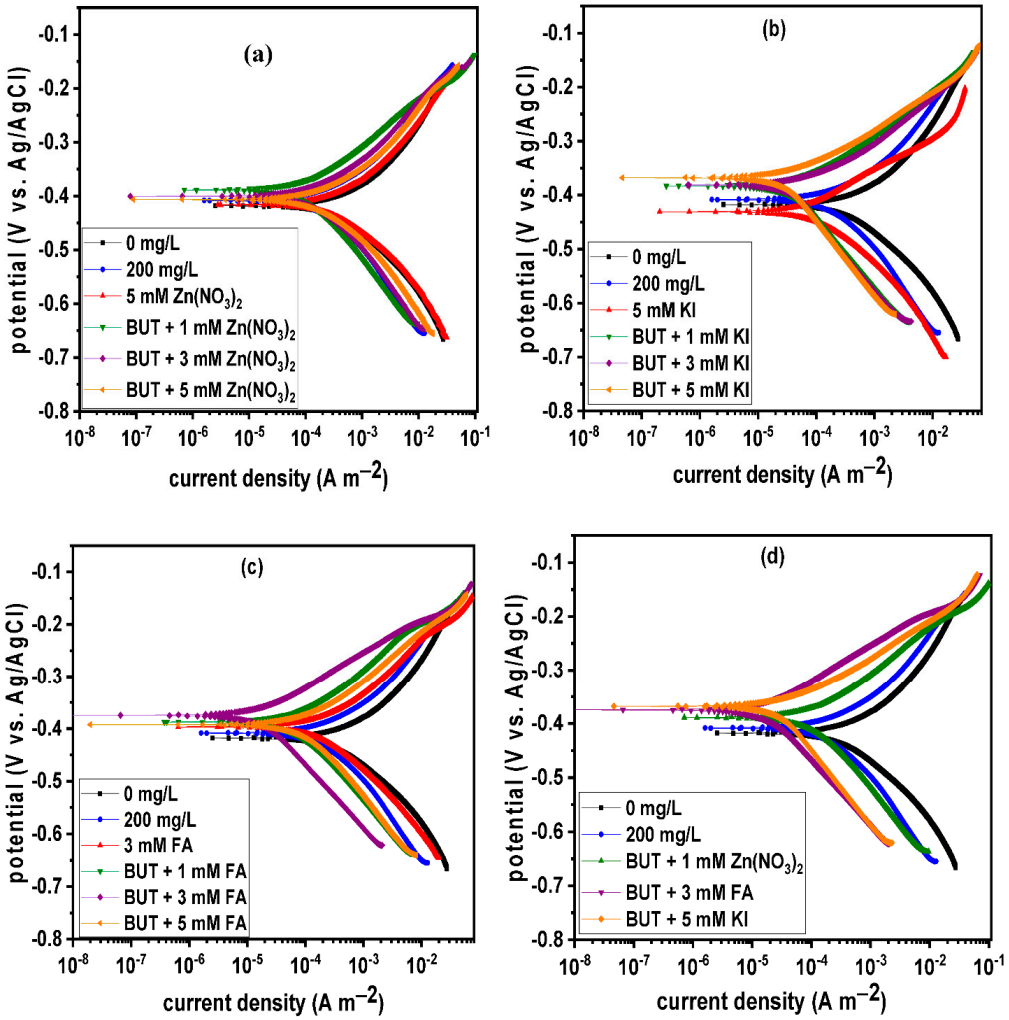

Figure 4. Potentiodynamic polarization curves for API 5L X60 carbon steel at 25 °C in 15 wt.% HCl solution without and with best performing concentration of synergist, 200 mg/L BUT alone and in combination with different concentrations of (**a**) $Zn(NO_3)_2$, (**b**) KI, (**c**) formic acid (FA) and (**d**) comparison of the best BUT + synergist combination.

Table 4. Polarization parameters obtained during acid corrosion of API 5L carbon steel in 15 wt.% HCl solution without and with 200 ppm BUT alone and in combination with different synergists at 25 °C.

System	LPR		PDP						
	Rp (Ω cm^2)	% η_{LPR}	$-E_{corr}$ (mV/Ag/AgCl)	i_{corr} (μA cm^{-2})	β_a (mV dec^{-1})	$-\beta_c$ (mV dec^{-1})	f_a	f_c	% η_{PDP}
200 ppm BUT	122.40 ± 1.40	49.12	416	255.60	107.00	122.10	0.51	0.50	50.35
BUT + 1 mM FA	341.10 ± 1.05	81.74	388	82.04	92.40	136.50	0.22	0.20	84.07
BUT + 3 mM FA	1035.00 ± 2.75	93.98	374	15.96	66.60	119.00	0.06	0.04	96.90
BUT + 5 mM FA	269.00 ± 1.56	76.85	393	104.55	89.50	138.90	0.27	0.24	79.69
BUT + 1 mM KI	473.30 ± 1.57	86.84	384	33.12	58.30	128.40	0.12	0.08	93.57
BUT + 3 mM KI	376.70 ± 3.02	83.47	383	34.13	48.60	137.50	0.14	0.09	93.37
BUT + 5 mM KI	641.90 ± 2.90	90.30	368	25.96	55.30	139.20	0.12	0.07	94.96
BUT + 1 mM $Zn(NO_3)_2$	240.90 ± 4.44	74.15	388	112.16	84.80	137.30	0.31	0.27	78.22
BUT + 3 mM $Zn(NO_3)_2$	155.70 ± 2.31	60.01	400	209.14	92.20	141.10	0.49	0.46	59.37
BUT + 5 mM $Zn(NO_3)_2$	120.10 ± 1.21	48.15	407	306.17	108.70	136.10	0.66	0.64	40.53

The observed improvement in BUT inhibition performance upon combination with the selected intensifiers could be due to a synergy in the adsorption of phytoconstituents of BUT and the intensifiers. Normally, the synergism parameter (S_θ) (it can be calculated using Equation (10) [39]) is used to categorize co-adsorption as synergistic or antagonistic [39]. If $S_\theta > 1$, it signifies synergistic effect, that is, cooperative adsorption whereas $S_\theta < 1$ is indicative of antagonistic effect, i.e., competitive adsorption [39].

$$S_\theta = \frac{1 - (\theta_1 + \theta_2 - \theta_1\theta_2)}{1 - \theta^1_{1+2}} \quad (10)$$

where θ_1 = the degree of surface coverage of BUT, θ_2 = the degree of surface coverage of intensifier alone and θ^1_{1+2} = the degree of surface coverage of BUT + intensifier mixtures. The degree of surface coverage is calculated from Equation (11) [39]. In this study, η data from EIS techniques are used.

$$\theta = \frac{\eta}{100} \quad (11)$$

Figure 5 shows the plot of S_θ against the BUT + intensifiers concentrations. It is clear that all the studied concentrations of FA and KI produced synergistic effect with BUT. As could be seen the S_θ values are more than unity for BUT + FA and BUT + KI combination. The implication is that BUT + KI and BUT + FA mixtures cooperatively adsorbed on the carbon steel surface [39,43,50], that is BUT molecules adsorbed on iodide ions or CO adsorbed layer. In the case of $Zn(NO_3)_2$, a synergy is noticed between BUT and 1 mM $Zn(NO_3)_2$ but the effect diminished with increasing concentration of $Zn(NO_3)_2$ and at 5 mM, a completely antagonistic behavior is observed (S_θ = 0.94). This explains the behavior of $Zn(NO_3)_2$ noted in Figures 3a and 4a. The saturation of the corrosion systems containing the higher concentrations of $Zn(NO_3)_2$ may have caused the species to compete for adsorption and as effect imparted negatively on the inhibition performance.

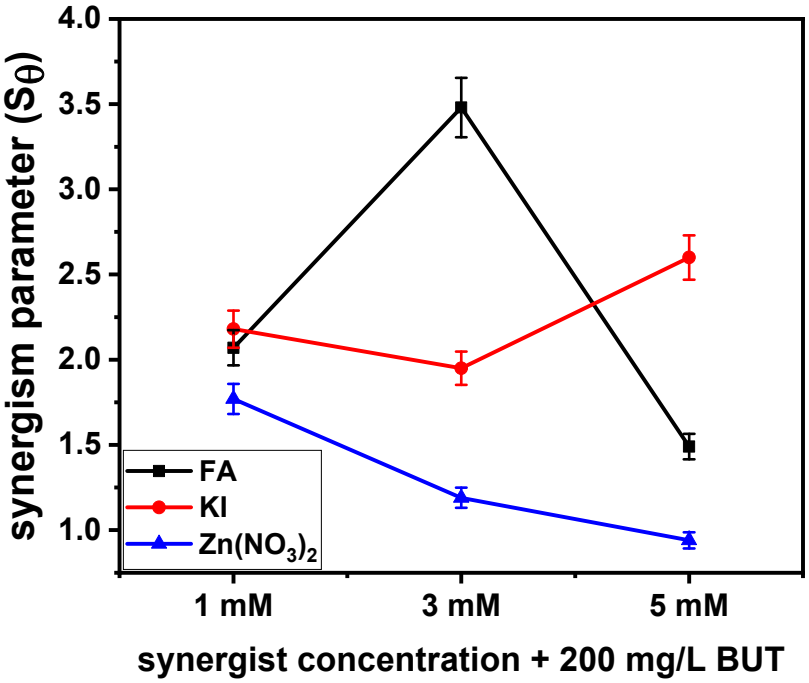

Figure 5. The variation of the calculated synergism parameter with BUT + synergist concentration.

3.3. Effect of Temperature On Corrosion Rate and Corrosion Inhibition

The classical mass loss measurement technique was adopted for the study of the influence of temperature on the corrosion rate of API 5L X60 carbon steel in 15 wt.% HCl solution and on the inhibition efficacy of BUT alone and BUT + intensifiers mixtures. For these sets of experiments, 200 mg/L BUT, BUT + 1 mM $Zn(NO_3)_2$, BUT + 3 mM FA, and BUT + 5 mM KI (i.e., best performing mixtures) were considered. Figure 6 shows the variation of (a) corrosion rate and (b) inhibition efficiency with temperature. It is obvious in Figure 6a that temperature promoted the dissolution of the carbon steel in both uninhibited and inhibited acid solutions. As could be seen, the corrosion rate increases with rise in temperature. This observation is not surprising considering the fact that an increase in temperature causes a rise in energy levels of molecules involved in a reaction [51]. Nevertheless, the rate of corrosion was significantly suppressed in the inhibited acid solutions with BUT + 3 mM FA and BUT + 5 mM KI producing the most profound effect. At 60 °C, the presence of BUT + 3 mM FA and BUT + 5 mM KI in the acid solution reduced the corrosion rate of API 5L X60 carbon steel from 430.60 $\times$ 10^{-5} g cm^{-2} h^{-1} to 63.29 $\times$ 10^{-5} g cm^{-2} h^{-1} and 67.94 $\times$ 10^{-5} g cm^{-2} h^{-1}, respectively, and this corresponded to corrosion inhibition efficiency of 85.30% and 84.22% (Figure 6b). An interesting observation is made upon inspection of Figure 6b. While a sharp decline in the corrosion inhibition efficiency of BUT and BUT + $Zn(NO_3)_2$ is observed, the inhibition efficiency of BUT + FA and BUT + KI mixtures relatively remains constant with rise in temperature. It appears that BUT and BUT + $Zn(NO_3)_2$ physically interacted with the carbon steel surface [52] while mixed adsorption mechanism describes the adsorption of BUT + FA and BUT + KI mixtures [53,54]. It is worth pointing out that, despite the slight decline in the inhibition efficiency of the BUT + FA and BUT + KI mixtures with rise in temperature, inhibition efficiency above 85% was still achieved. This again shows the potential of BUT + FA and BUT + KI mixtures in acting as acidizing corrosion inhibitors.

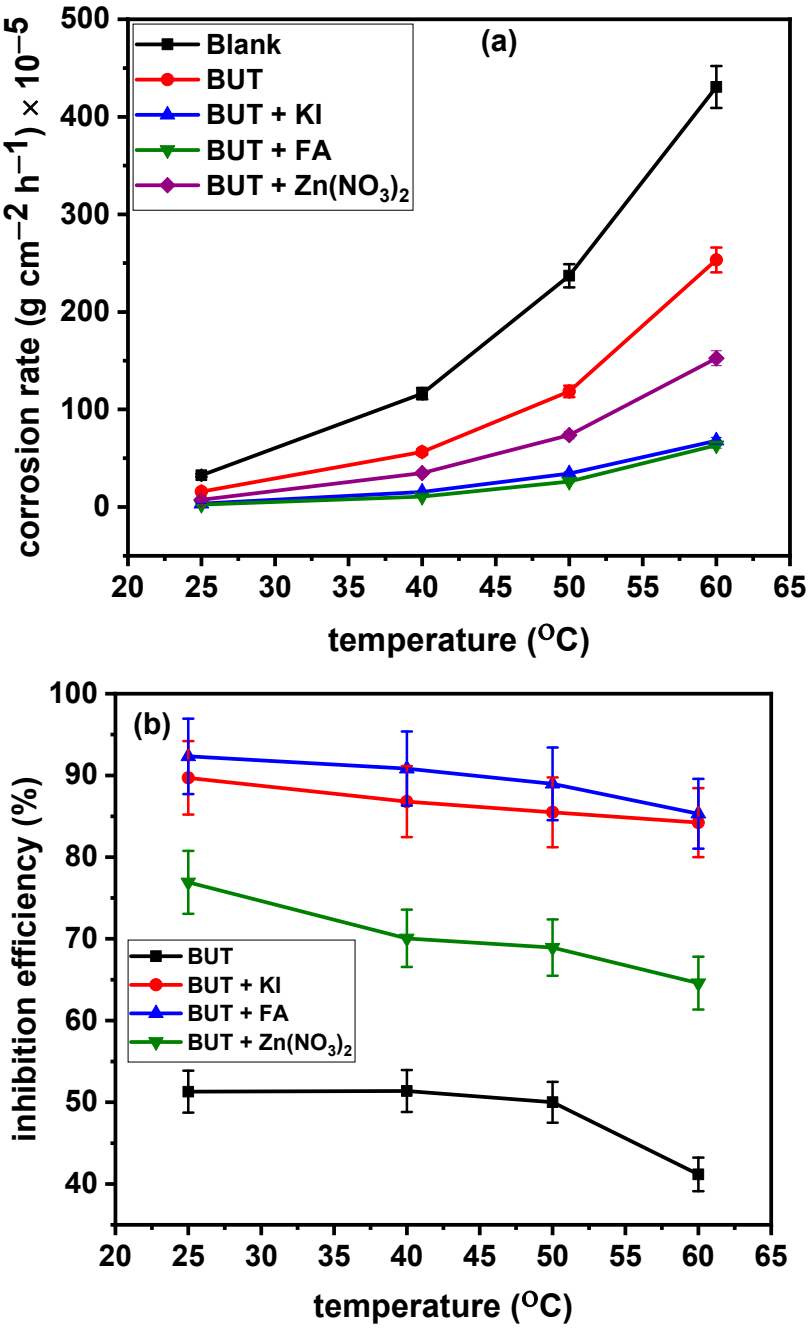

Figure 6. The variation of (**a**) corrosion rate and (**b**) inhibition efficiency with temperature for the corrosion of API 5L X60 carbon steel in 15 wt.% HCl solution devoid of and containing different additives from mass loss experiments.

3.4. Surface Analysis

3.4.1. SEM and EDAX

The surfaces of API 5L X60 carbon steel samples immersed in 15 wt.% HCl solution (a) without and with (b) 200 mg/L BUT extract, (c) 200 mg/L BUT + 3 mM FA, (d) 200 mg/L BUT + 5 mM KI, (e) 200 mg/L BUT + 1 mM $Zn(NO_3)_2$ for 24 h at 25 °C were examined using SEM (Figure 7). The composition of the deposits on the entire surfaces were determined using EDAX (Figure 8). Upon immersion of the abraded metal sample in 15 wt.% HCl solution, serious corrosion that resulted in the damaged and rough morphology seen in Figure 7a occurred. A heap of loosely adhered corrosion products with a salt-like appearance is observed on the surface (Figure 7a). Previous works [41] had shown that iron

chloride salt is one of the products during the corrosion of carbon steel in HCl environment. The EDAX results in Figure 8a confirms the presence of chloride on the surface. In contrast, the surface in Figure 7b is smoother and more compact agreeing with the other experimental results (Table 1) that BUT inhibited the corrosion API 5L X60 carbon steel in 15 wt.% HCl solution. The Cl content in Figure 8a (8.5%) significantly reduced in Figure 8b (4.7%) suggesting less corrosion probably due to BUT phytoconstituents adsorption. However, some cavities can still be spotted on the surface in Figure 7b meaning that, BUT alone did not appreciably protect the steel surface from corrosion. From electrochemical experimental studies (Table 1), the 200 mg/L BUT only protected the metal surface by approximately 50%. By comparing the surfaces in Figure 7c,d to the one in Figure 7b, it could be said that the BUT + FA and BUT + KI mixtures highly protected the metal surface. The surfaces in Figure 7c,d are completely covered with firmly adhered products. The BUT + FA surface (Figure 7c) seems most protected. The EDAX spectra in Figure 8c,d reveals that chloride content was less on these surfaces. A different observation is, however, made on inspecting the micrograph of the surface protected with BUT + $Zn(NO_3)_2$ mixture (Figure 7e. Loosely adhered jelly-like products are seen on the surface and the EDAX spectrum in Figure 8e reveals that this surface relative to the surfaces in Figure 8c,d has the highest chloride content. This confirms the other experimental results (Tables 3 and 4) that the BUT + $Zn(NO_3)_2$ mixture is not suited for the studied conditions.

3.4.2. AFM

A detailed visualization of an examined sample surface can be achieved by AFM since it can produce a three-dimensional (3-D) image. A surface with the highest roughness is always adjudged to indicate a severe corrosion attack [30,52]. The 2-D and 3-D images of API 5L X60 carbon steel samples after exposing to 15 wt.% HCl solution (a) without and with (b) 200 mg/L BUT extract, (c) 200 mg/L BUT + 3 mM FA, (d) 200 mg/L BUT + 5 mM KI, (e) 200 mg/L BUT + 1 mM $Zn(NO_3)_2$ for 24 h at 25 °C are shown in Figure 9. Obviously, the carbon steel surface exposed to the uninhibited acid solution (Figure 9a) exhibited the roughest topography relative to the surfaces shown in Figure 9b–e. The AFM also gives information in terms of surface roughness and the average value of profile deviation from the mean line (R_a) is one useful parameter that can be used to adjudge the extent of corrosion on a corroding surface [39]. In the present case, R_a for the unprotected carbon steel surface, carbon steel surfaces protected with 200 mg/L BUT, BUT + 3 mM FA, BUT + 5 mM KI, and BUT + 1 mM $Zn(NO_3)_2$ is 0.087 μm, 0.013 μm, 0.038 μm, 0.043 μm, and 0.058 μm, respectively. The lesser R_a values for protected API 5L X60 carbon steel surfaces in comparison with the R_a value of the unprotected surface is most probably due to surface protection occasioned by the adsorption of the inhibitors. The smaller R_a values for BUT + FA (0.038 μm) and BUT + KI (0.043 μm) compare to that of BUT + $Zn(NO_3)_2$ (0.058 μm) protected surfaces again confirm that BUT + FA and BUT + KI mixtures are more efficient corrosion inhibitor than BUT + $Zn(NO_3)_2$ mixture.

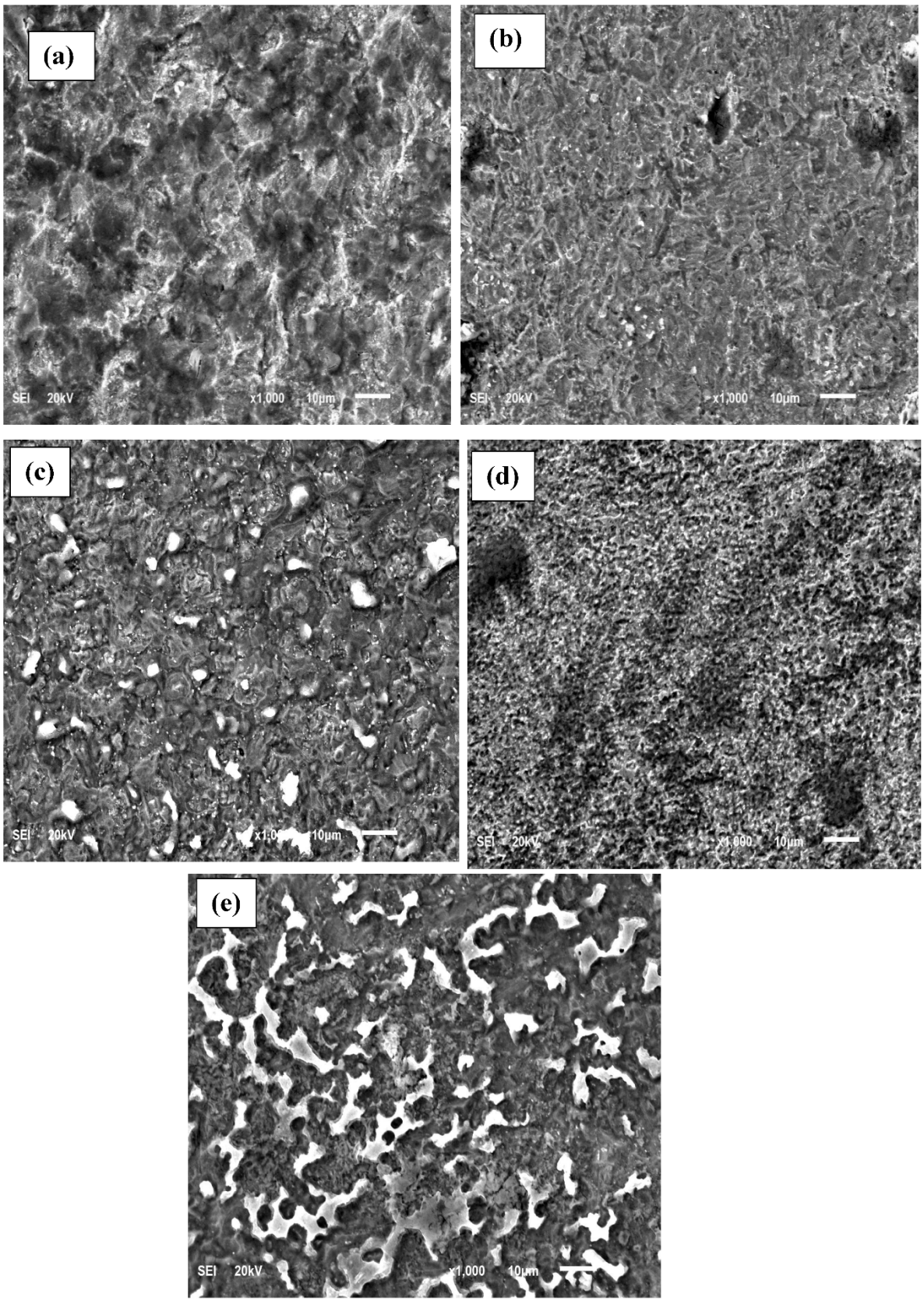

Figure 7. SEM images of API 5L X60 carbon steel at 25 °C after immersion in 15 wt.% HCl solution (**a**) without inhibitor, and containing (**b**) 200 mg/L BUT extract, (**c**) 200 mg/L BUT + 3 mM FA, (**d**) 200 mg/L BUT + 5 mM KI, (**e**) 200 mg/L BUT + 1 mM $Zn(NO_3)_2$ for 24 h.

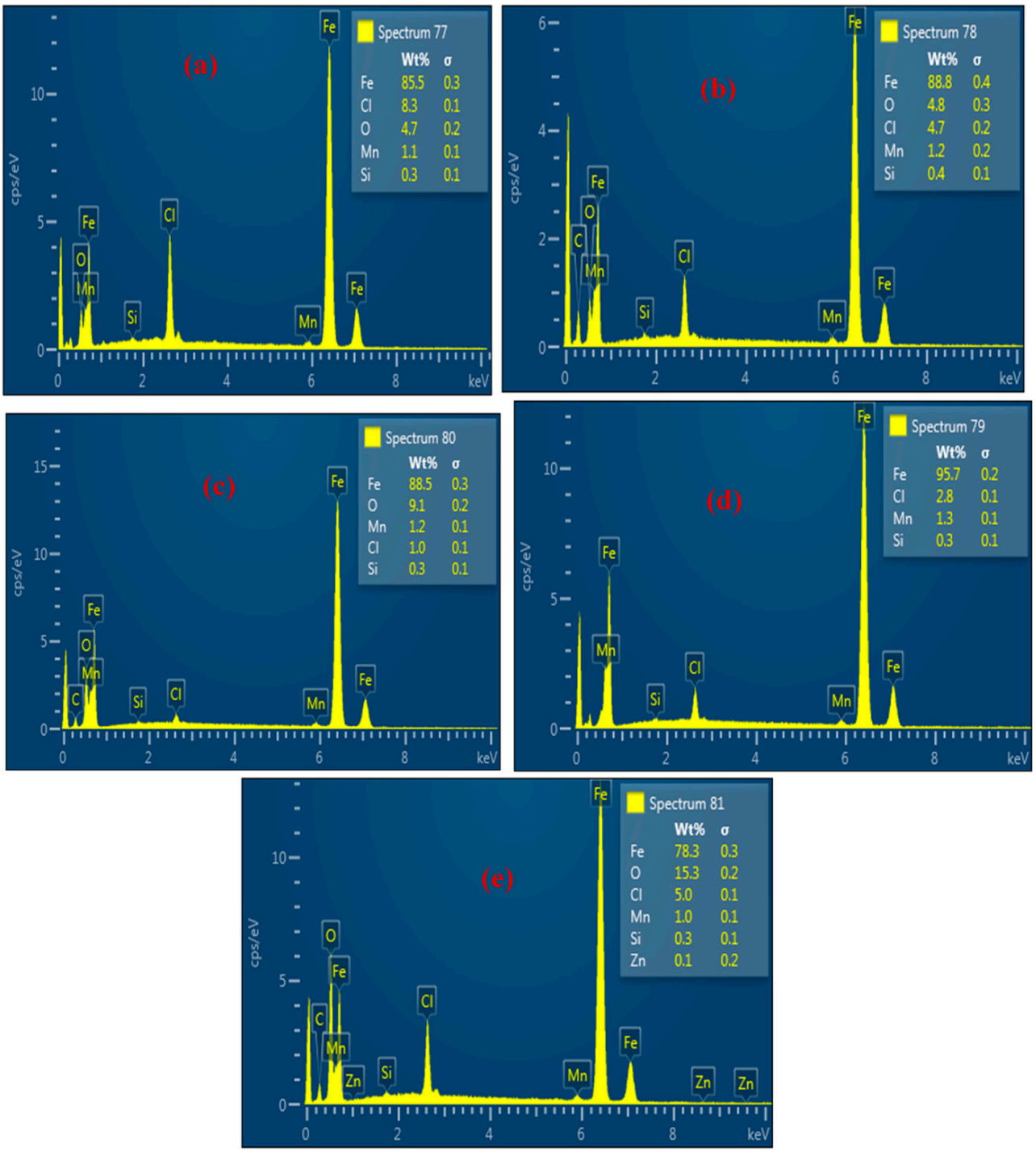

Figure 8. EDAX spectra of API 5L X60 carbon steel at 25 °C after immersion in 15 wt.% HCl solution (**a**) without inhibitor, and containing (**b**) 200 mg/L BUT extract, (**c**) 200 mg/L BUT + 3 mM FA, (**d**) 200 mg/L BUT + 5 mM KI, (**e**) 200 mg/L BUT + 1 mM $Zn(NO_3)_2$ for 24 h.

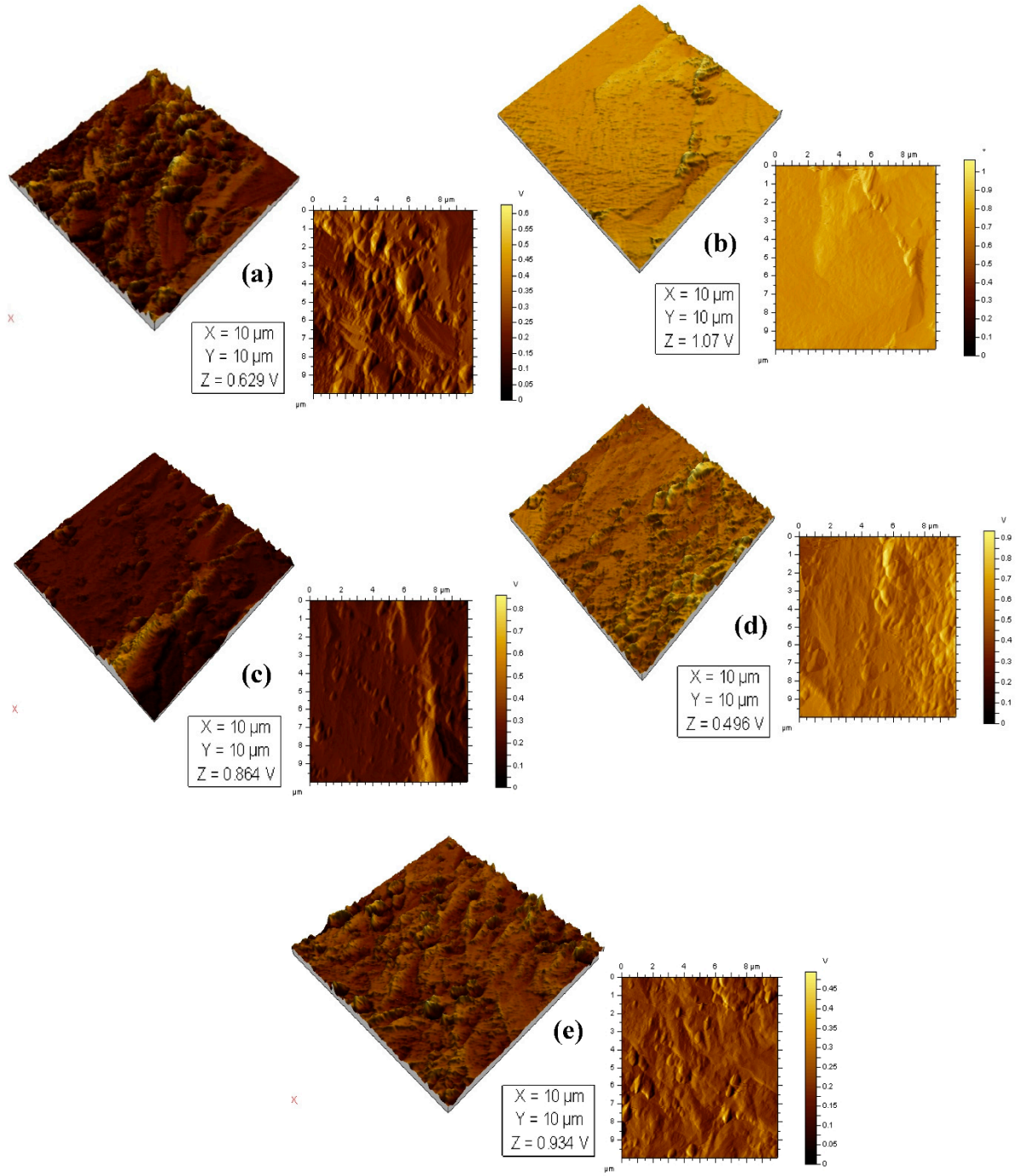

Figure 9. AFM micrographs of API 5L X60 carbon steel at 25 °C after immersion in 15 wt.% HCl solution (**a**) without inhibitor, and containing (**b**) 200 mg/L BUT extract, (**c**) 200 mg/L BUT + 3 mM FA, (**d**) 200 mg/L BUT + 5 mM KI, (**e**) 200 mg/L BUT + 1 mM $Zn(NO_3)_2$ for 24 h.

4. Conclusions and Outlook

The corrosion inhibition performance of butanolic date palm leaves extract (BUT) on API 5L X60 carbon steel dissolution in 15 wt.% HCl solution was studied. The effect of intensifiers, namely formic acid (FA), potassium iodide (KI), and zinc nitrate ($Zn(NO_3)_2$) as well as temperature on the corrosion inhibiting performance of BUT was also investigated. From the studies, the following conclusions are drawn:

1. BUT has the potential to serve as an active in corrosion inhibitor package developed for carbon steel protection in an acidizing environment;

2. FA and KI at appropriate concentration can be utilized as intensifier for BUT. With 200 mg/L BUT + 3 mM FA and 200 mg/L BUT + 5 mM KI, inhibition efficiency of 97% and 95%, respectively can be realized at normal temperature;
3. $Zn(NO_3)_2$ is not a suitable intensifier for BUT under acidizing conditions;
4. The adsorption of BUT + FA and BUT + KI is synergistic in nature;
5. BUT alone and in combination with the selected intensifiers act as a mixed-type corrosion inhibition inhibiting both the anodic and cathodic corrosion reactions;
6. Increase in the temperature of the acid solution would cause a slight decline in the inhibition efficiency of BUT + FA and BUT + KI but inhibition efficiency of above 85% is achievable at 60 °C;
7. The SEM and AFM confirm that BUT + FA and BUT + KI are effective in inhibiting the corrosion of API 5L X60 carbon steel in 15 wt.% HCl solution.

Although the use of plant parts extracts as corrosion inhibitors is advantageous because of certain properties such as eco-friendliness, biodegradability, renewability, and low-cost when compared to synthetic organic and inorganic corrosion inhibitors, there are still some unanswered questions regarding the use of plant extracts as metals corrosion inhibitor. The primary criticism is on the inability of scientists to pinpoint on the specific component(s) that is/are responsible for the inhibition of corrosion given that a plant extract contains multiple phytochemical compounds. In our present study, the pertinent questions are: why are butanol extracts performing better than others and which compound(s) is/are responsible for it? To provide answers to these questions, we recently acquired a state-of-the-art preparative HPLC-MS instrument from Agilent Technologies, USA. Work is ongoing using this equipment to isolate the compound(s) present in the BUT that is/are responsible for the observed corrosion inhibition effect.

Author Contributions: Conceptualization, S.A.U., I.B.O., and R.K.S.; methodology, S.A.U., I.B.O., R.K.S., and M.M.S.; validation, S.A.U., I.B.O., R.K.S., and M.M.S.; formal analysis, S.A.U., and M.M.S.; investigation, S.A.U., I.B.O., R.K.S., and M.M.S.; data curation, S.A.U., I.B.O., R.K.S., and M.M.S.; writing—original draft preparation, M.M.S.; writing—review and editing, S.A.U., I.B.O., R.K.S., and M.M.S.; project administration, S.A.U.; funding acquisition, S.A.U. All authors have read and agreed to the published version of the manuscript.

Funding: This work was funded by the King Abdul-Aziz City for Science and Technology (KACST) under the National Science Technology Plan (NSTIP) grant No. 14-ADV2452-04.

Institutional Review Board Statement: Not applicable.

Informed Consent Statement: Not applicable.

Data Availability Statement: Data will be provided upon request.

Acknowledgments: Authors acknowledge the support received from King Abdul-Aziz City for Science and Technology (KACST) for funding this work under the National Science Technology Plan (NSTIP) grant No. 14-ADV2452-04. The support provided by the Deanship of Scientific Research (DSR) and the Center of Research Excellence in Corrosion (CORE-C) at King Fahd University of Petroleum and Minerals (KFUPM) is also acknowledged.

Conflicts of Interest: The authors declare no conflict of interest.

References

1. Global Oil & Gas Exploration & Production—Industry Data, Trends, Stats | IBISWorld. Available online: https://www.ibisworld.com/global/market-research-reports/global-oil-gas-exploration-production-industry/ (accessed on 3 February 2021).
2. Oil & Gas | Blackmer. Available online: https://www.psgdover.com/blackmer/markets/oil-gas (accessed on 3 February 2021).
3. Obot, I.B.; Solomon, M.M.; Umoren, S.A.; Suleiman, R.; Elanany, M.; Alanazi, N.M.; Sorour, A.A. Progress in the development of sour corrosion inhibitors: Past, present, and future perspectives. *J. Ind. Eng. Chem.* **2019**, *79*, 1–18. [CrossRef]
4. Umoren, S.A.; Solomon, M.M. Protective polymeric films for industrial substrates: A critical review on past and recent applications with conducting polymers and polymer composites/nanocomposites. *Prog. Mater. Sci.* **2019**, *104*, 380–450. [CrossRef]
5. Cao, S.; Liu, D.; Ding, H.; Wang, J.; Lu, H.; Gui, J. Task-specific ionic liquids as corrosion inhibitors on carbon steel in 0.5 M HCl solution: An experimental and theoretical study. *Corros. Sci.* **2019**, *153*, 301–313. [CrossRef]

6. Onyeachu, I.B.; Obot, I.B.; Sorour, A.A.; Abdul-Rashid, M.I. Green corrosion inhibitor for oilfield application I: Electrochemical assessment of 2-(2-pyridyl) benzimidazole for API X60 steel under sweet environment in NACE brine ID196. *Corros. Sci.* **2019**, *150*, 183–193. [CrossRef]
7. Umoren, S.A.; Solomon, M.M. Polymeric Corrosion Inhibitors for Oil and Gas Industry. In *Corrosion Inhibitors in the Oil and Gas Industry*; Umoren, S.A., Saji, V.S., Eds.; Wiley: Hoboken, NJ, USA, 2020; pp. 303–320.
8. Singh, A.; Quraishi, M.A. Acidizing Corrosion Inhibitors: A Review. *J. Mater. Environ. Sci* **2015**, *6*, 224–235.
9. Alhaffar, M.T.; Umoren, S.A.; Obot, I.B.; Ali, S.A.; Solomon, M.M. Studies of the anticorrosion property of a newly synthesized Green isoxazolidine for API 5L X60 steel in acid environment. *J. Mater. Res. Technol.* **2019**, *8*, 4399–4416. [CrossRef]
10. Zhang, Q.H.; Hou, B.S.; Li, Y.Y.; Zhu, G.Y.; Liu, H.F.; Zhang, G.A. Two novel chitosan derivatives as high efficient eco-friendly inhibitors for the corrosion of mild steel in acidic solution. *Corros. Sci.* **2019**, *164*, 108346. [CrossRef]
11. Umoren, S.A.; Solomon, M.M. Synergistic corrosion inhibition effect of metal cations and mixtures of organic compounds: A Review. *J. Environ. Chem. Eng.* **2016**, *5*, 246–273. [CrossRef]
12. Obot, I.B.; Solomon, M.M.; Onyeachu, I.B.; Umoren, S.A.; Meroufel, A.; Alenazi, A.; Sorour, A.A. Development of a green corrosion inhibitor for use in acid cleaning of MSF desalination plant. *Desalination* **2020**, *495*, 114675. [CrossRef]
13. Marciales, A.; Haile, T.; Ahvazi, B.; Ngo, T.D.; Wolodko, J. Performance of green corrosion inhibitors from biomass in acidic media. *Corros. Rev.* **2018**, *36*, 239–266. [CrossRef]
14. Lerner, S. Europeans Aim to Phase Out Toxic PFAS Chemicals by 2030. Available online: https://theintercept.com/2019/12/19/pfas-chemicals-europe-phase-out/ (accessed on 6 October 2020).
15. Haque, J.; Verma, C.; Srivastava, V.; Nik, W.B.W. Corrosion inhibition of mild steel in 1M HCl using environmentally benign Thevetia peruviana flower extracts. *Sustain. Chem. Pharm.* **2021**, *19*, 100354. [CrossRef]
16. Haldhar, R.; Prasad, D.; Mandal, N.; Benhiba, F.; Bahadur, I.; Dagdag, O. Colloids and Surfaces A: Physicochemical and Engineering Aspects Anticorrosive properties of a green and sustainable inhibitor from leaves extract of Cannabis sativa plant: Experimental and theoretical approach. *Colloids Surf. A Physicochem. Eng. Asp.* **2021**, *614*, 126211. [CrossRef]
17. Zuo, X.; Li, W.; Luo, W.; Zhang, X.; Qiang, Y.; Zhang, J.; Li, H.; Tan, B. Research of Lilium brownii leaves extract as a commendable and green inhibitor for X70 steel corrosion in hydrochloric acid. *J. Mol. Liq.* **2021**, *321*, 114914. [CrossRef]
18. Tan, B.; He, J.; Zhang, S.; Xu, C.; Chen, S.; Liu, H.; Li, W. Insight into anti-corrosion nature of Betel leaves water extracts as the novel and eco-friendly inhibitors. *J. Colloid Interface Sci.* **2021**, *585*, 287–301. [CrossRef] [PubMed]
19. Farhadian, A.; Rahimi, A.; Safaei, N.; Shaabani, A.; Abdouss, M.; Alavi, A. A theoretical and experimental study of castor oil-based inhibitor for corrosion inhibition of mild steel in acidic medium at elevated temperatures. *Corros. Sci.* **2020**, *175*, 108871. [CrossRef]
20. Umoren, S.A.; Solomon, M.M.; Obot, I.B.; Suleiman, R.K. A critical review on the recent studies on plant biomaterials as corrosion inhibitors for industrial metals. *J. Ind. Eng. Chem.* **2019**, *76*, 91–115. [CrossRef]
21. Umoren, S.A.; Solomon, M.M. Effect of halide ions on the corrosion inhibition efficiency of different organic species—A review. *J. Ind. Eng. Chem.* **2015**, *21*, 81–100. [CrossRef]
22. Finšgar, M.; Jackson, J. Application of corrosion inhibitors for steels in acidic media for the oil and gas industry: A review. *Corros. Sci.* **2014**, *86*, 17–41. [CrossRef]
23. Feng, L.; Zhang, S.; Lu, Y.; Tan, B.; Chen, S.; Guo, L. Synergistic corrosion inhibition effect of thiazolyl-based ionic liquids between anions and cations for copper in HCl solution. *Appl. Surf. Sci.* **2019**, *483*, 901–911. [CrossRef]
24. Loto, C.A.; Loto, R.T.; Popoola, A.P.I. Synergistic effect of tobacco and kola tree extracts on the corrosion inhibition of mild steel in acid chloride. *Int. J. Electrochem. Sci.* **2011**, *6*, 3830–3843.
25. Obot, I.B.; Madhankumar, A. Synergistic effect of iodide ion addition on the inhibition of mild steel corrosion in 1 M HCl by 3-amino-2-methylbenzylalcohol. *Mater. Chem. Phys.* **2016**, *177*, 266–275. [CrossRef]
26. Al-Katheeri, M.I.; Nasr-El-Din, H.A.; Taylor, K.C.; Al-Grainees, A.H. Determination and Fate of Formic Acid in High Temperature Acid Stimulation Fluids. In Proceedings of the International Symposium and Exhibition on Formation Damage Control, Lafayette, LA, USA, 20–21 February 2002; pp. 469–476.
27. Cassidy, J.M.; McNeil, R.I.; Kiser, C.E. Understanding formic acid decomposition as a corrosion inhibitor intensifier in strong acid environments. In Proceedings of the International Symposium on Oilfield Chemistry, Houston, TX, USA, 28 February–2 March 2007; pp. 422–430.
28. Farag, A.A.; Hegazy, M.A. Synergistic inhibition effect of potassium iodide and novel Schiff bases on X65 steel corrosion in 0.5 M H_2SO_4. *Corros. Sci.* **2013**, *74*, 168–177. [CrossRef]
29. Zhang, W.; Li, H.J.; Liu, Y.; Wang, D.; Chen, L.; Xie, L.; Li, L.; Zhang, W.; Wu, Y.C. Stevioside–Zn^{2+} system as an eco-friendly corrosion inhibitor for C1020 carbon steel in hydrochloric acid solution. *Colloids Surf. A Physicochem. Eng. Asp.* **2021**, *612*, 126010. [CrossRef]
30. Alinejad, S.; Naderi, R.; Mahdavian, M. Effect of inhibition synergism of zinc chloride and 2-mercaptobenzoxzole on protective performance of an ecofriendly silane coating on mild steel. *J. Ind. Eng. Chem.* **2017**, *48*, 88–98. [CrossRef]
31. Al-Redhaiman, K.N. Date Palm cultivation in Saudi Arabia: Current status and future prospects for development. In Proceedings of the ASHS Annual Conference, Orlando, FL, USA, 28–31 July 2014.
32. Nabili, A.; Fattoum, A.; Passas, R.; Elaloui, E. Extraction and characterization of cellulose from Date Palm seeds (*Phoenix dactylifera* L.). *Cellul. Chem. Technol.* **2016**, *50*, 1015–1023.

33. Nasser, R.A.; Salem, M.Z.M.; Hiziroglu, S.; Al-Mefarrej, H.A.; Mohareb, A.S.; Alam, M.; Aref, I.M. Chemical analysis of different parts of date palm (*Phoenix dactylifera* L.) using ultimate, proximate and thermo-gravimetric techniques for energy production. *Energies* **2016**, *9*, 374. [CrossRef]
34. ASTM. *G.-90. Standard Practice for Preparing, Cleaning, and Evaluating Corrosion Test Specimens*; ASTM: West Conshohocken, PA, USA, 2017.
35. NACE International. *TM0193-2016-SG Laboratory Corrosion Testing of Metals in Static Chemical Cleaning Solutions at Temperatures below 93 °C (200 °F)*; NACE International: Houston, TX, USA, 2016.
36. Odewunmi, N.A.; Solomon, M.M.; Umoren, S.A.; Ali, S.A. Comparative studies of the corrosion inhibition efficacy of a dicationic monomer and its polymer against API X60 steel corrosion in simulated acidizing fluid under static and hydrodynamic conditions. *ACS Omega* **2020**, *5*, 27057–27071. [CrossRef] [PubMed]
37. ASTM G3-89 Conventions applicable to electrochemical measurements in corrosion testing. In *Annual Book of ASTM Standard*; ASTM: West Conshohocken, PA, USA, 1994; Volume 30.
38. ASTM G3-94 Making potentiostatic and potentiodynamic anodic polarization measurements. In *Annual Book of ASTM Standard*; ASTM: West Conshohocken, PA, USA, 1994; Volume 48.
39. Solomon, M.M.; Umoren, S.A.; Obot, I.B.; Sorour, A.A.; Gerengi, H. Exploration of Dextran for Application as Corrosion Inhibitor for Steel in Strong Acid Environment: Effect of Molecular Weight, Modification, and Temperature on Efficiency. *ACS Appl. Mater. Interfaces* **2018**, *10*, 28112–28129. [CrossRef] [PubMed]
40. Dickson, O.; Goodluck, O.; Onyekpe, B.O. Corrosion inhibition for alloy 304L (UNS S30403) in H_2SO_4 1 M solution by *Centrosema pubescens* leaves extract. *Appl. Surf. Sci. Adv.* **2021**, *3*, 100061.
41. Kousar, K.; Walczak, M.S.; Ljungdahl, T.; Wetzel, A.; Oskarsson, H.; Restuccia, P.; Ahmad, A.; Harrison, N.M.; Lindsay, R. Corrosion inhibition of carbon steel in hydrochloric acid: Elucidating the performance of an imidazoline-based surfactant. *Corros. Sci.* **2021**, *180*, 109195. [CrossRef]
42. Brug, G.J.; van den Eeden, A.L.G.; Sluyters-Rehbach, M.; Sluyters, J.H. The analysis of electrode impedances complicated by the presence of a constant phase element. *J. Electroanal. Chem.* **1984**, *176*, 275–295. [CrossRef]
43. Solomon, M.M.; Umoren, S.A.; Quraishi, M.A.; Tripathi, D.; Abai, E.J. Effect of akyl chain length, flow, and temperature on the corrosion inhibition of carbon steel in a simulated acidizing environment by an imidazoline-based inhibitor. *J. Pet. Sci. Eng.* **2020**, *187*, 106801. [CrossRef]
44. Luo, X.; Ci, C.; Li, J.; Lin, K.; Du, S.; Zhang, H.; Li, X.; Cheng, Y.F.; Zang, J.; Liu, Y. 4-aminoazobenzene modified natural glucomannan as a green eco-friendly inhibitor for the mild steel in 0.5 M HCl solution. *Corros. Sci.* **2019**, *151*, 132–142. [CrossRef]
45. Gerengi, H.; Sen, N.; Uygur, I.; Solomon, M.M.M. Corrosion response of ultra-high strength steels used for automotive applications. *Mater. Res. Express* **2019**, *6*, 0865a6. [CrossRef]
46. Arellanes-Lozada, P.; Díaz-Jiménez, V.; Hernández-Cocoletzi, H.; Nava, N.; Olivares-Xometl, O.; Likhanova, N.V. Corrosion inhibition properties of iodide ionic liquids for API 5L X52 steel in acid medium. *Corros. Sci.* **2020**, *175*, 108888. [CrossRef]
47. Honarvar Nazari, M.; Shihab, M.S.; Havens, E.A.; Shi, X. Mechanism of corrosion protection in chloride solution by an apple-based green inhibitor: Experimental and theoretical studies. *J. Infrastruct. Preserv. Resil.* **2020**, *1*, 7. [CrossRef]
48. Cao, C. On electrochemical techniques for interface inhibitor research. *Corros. Sci.* **1996**, *38*, 2073–2082. [CrossRef]
49. Umoren, S.A.; Solomon, M.M.; Udosoro, I.I.; Udoh, A.P. Synergistic and antagonistic effects between halide ions and carboxymethyl cellulose for the corrosion inhibition of mild steel in sulphuric acid solution. *Cellulose* **2010**, *17*, 635–648. [CrossRef]
50. Solomon, M.M.; Umoren, S.A.; Quraishi, M.A.; Salman, M. Myristic acid based imidazoline derivative as effective corrosion inhibitor for steel in 15% HCl medium. *J. Colloid Interface Sci.* **2019**, *551*, 47–60. [CrossRef]
51. Petrucci, R.; Herring, F.; Madura, J.; Bissonnette, C. *General Chemistry: Principles and Modern Applications, Loose Leaf Version*, 10th ed.; Pearson Prentice Hall: Hoboken, NJ, USA, 2010; ISBN 978-0132064521.
52. Paul, P.K.; Yadav, M. Investigation on corrosion inhibition and adsorption mechanism of triazine-thiourea derivatives at mild steel/HCl solution interface: Electrochemical, XPS, DFT and Monte Carlo simulation approach. *J. Electroanal. Chem.* **2020**, *877*, 114599. [CrossRef]
53. Tao, Z.; He, W.; Wang, S.; Zhang, S.; Zhou, G. A study of differential polarization curves and thermodynamic properties for mild steel in acidic solution with nitrophenyltriazole derivative. *Corros. Sci.* **2012**, *60*, 205–213. [CrossRef]
54. Solomon, M.M.; Gerengi, H.; Kaya, T.; Umoren, S.A. Enhanced corrosion inhibition effect of chitosan for St37 in 15% H_2SO_4 environment by silver nanoparticles. *Int. J. Biol. Macromol.* **2017**, *104*, 638–649. [CrossRef] [PubMed]